

Cracking of brittle coatings adhesively bonded to substrates of unlike modulus

Kee Sung Lee, Young-Woo Rhee,^{a)} Douglas H. Blackburn,^{b)} and Brian R. Lawn
*Materials Science and Engineering Laboratory, National Institute of Standards and Technology,
Gaithersburg, Maryland 20899*

Herzl Chai
*Department of Solid Mechanics, Materials and Structures, Faculty of Engineering,
Tel Aviv University, Israel 69978*

(Received 10 March 2000; accepted 22 May 2000)

The role of elastic mismatch in determining critical conditions for indentation fracture in brittle coatings on substrates of unlike modulus was investigated. A model transparent trilayer system, consisting of a glass coating layer bonded to a thick substrate of different glass or polymer by a thin layer of epoxy adhesive, facilitated *in situ* observations of crack initiation and propagation. A tungsten carbide sphere was used to load the layer system. Abrasion flaws were introduced into the top and bottom glass coating surfaces to control the flaw populations and to predetermine the origins of fracture: cone cracks occurred at abraded top surfaces, radial cracks at abraded bottom surfaces. Analytical relations for the critical loads are presented for each crack system in terms of elastic modulus mismatch, indenter and coating dimensions, and material fracture parameters. Implications concerning materials selection for resistance to crack initiation are considered.

The problem of a brittle coating bonded to a substrate is of practical importance in layer applications. Engineering structures such as cutting tools, laminated windows and thermal barrier coatings, and natural structures like shells, teeth, and artificial crowns are examples. Hard outer layers provide resistance against damage from external influences (predominantly mechanical but also thermal and chemical); soft inner layers provide stress redistribution and crack containment. The adhesive needs to be sufficiently well bonded to the adjacent brittle layers to preclude delamination failures and soft enough to prevent sharp transverse cracks from penetrating into adjacent layers.

Such considerations are especially important in the case of cracks formed from contacts or impact at the outer coating surface. Unfortunately, a soft support also allows the coating to flex beneath the contact, leading to changes in coating fracture mode from surface cone crack to a more dangerous subsurface radial crack. Such transitions in crack mode have been well documented for brittle coatings fused to soft substrates.¹⁻¹³ *In situ* observations in a model transparent bilayer system consisting

of a soda-lime glass layer bonded to a plastic substrate have proved especially useful in describing such modes.¹⁴ Recently, we have examined a trilayer system in which an upper soda-lime glass layer (coating) is bonded to a like lower glass layer (substrate) with a soft epoxy adhesive.¹⁵ In that latter case it is the soft adhesive rather than the substrate that allows the flexure mode to develop and generate radial fractures.

Here we extend this last study to include substrates of different elastic modulus, in order to examine the influence of elastic mismatch in the sandwich structure. For this purpose we retain soda-lime glass as the top coating layer and the same epoxy as the adhesive but use different glasses and polymers as the substrate. We demonstrate a modest influence of substrate modulus on the critical conditions for contact-induced radial cracking.

Model transparent layer systems were constructed from rectangular glass plates 75 × 25 mm and indentation-tested according to the schematic in Fig. 1. Upper coating layers were soda-lime glass microscope slides of thickness $d = 1$ mm. Lower support layers were formed from different glass compositions or polymeric materials as slabs of thickness 12.5 mm. The latter glasses were prepared in-house from starting powder compositions (Table I). The polymers were a commercially available polycarbonate (AIN Plastics, Norfolk, VA), an acrylic (Lucite, ICI Acrylics, Wilmington, DE), and a softer plastic cut from a commercial plastic sheet. Young's

^{a)}Guest Scientist from Department of Materials Science and Engineering, Korea Advanced Institute of Science and Technology, Yusong, Taejon 305-701, Korea.

^{b)}Ceramics Division.

modulus was measured for each material using an acoustic impulse excitation apparatus (Grindosonic MK5, J.W. Lemmens Inc., St. Louis, MO) (Table I).

Either the top or the bottom glass surfaces of the upper glass layers were abraded with a slurry of 600 SiC grit, in order to provide a uniform density of flaws for crack initiation and to predetermine the crack mode.¹⁴ Opposite (nonabraded) surfaces were etched (12% hydrofluoric acid for 10 min), to reduce flaw severity on those surfaces. The upper and lower glass plates were then bonded together with epoxy adhesive (Harcos Chemicals, Bellesville, NJ) under light pressure, resulting in an interlayer thickness $h = 10 \pm 3 \mu\text{m}$ (measured by optical microscopy after sectioning).

Indentation tests were made with a tungsten carbide (WC) sphere of radius $r = 3.18 \text{ mm}$ at predetermined normal contact loads P , using a screw-driven testing machine (Instron 4501, Instron Corp., Canton, MA) at constant crosshead speed 0.2 mm min^{-1} . Subsurface contact regions in the coatings were viewed *in situ* from beneath the contacts using a Questar telescope (Questar, New Hope, PA). Precoating the top contact surface with a gold film enhanced the illumination. Critical loads P_{cone} to produce surface cone cracks, or P_{rad} to produce subsur-

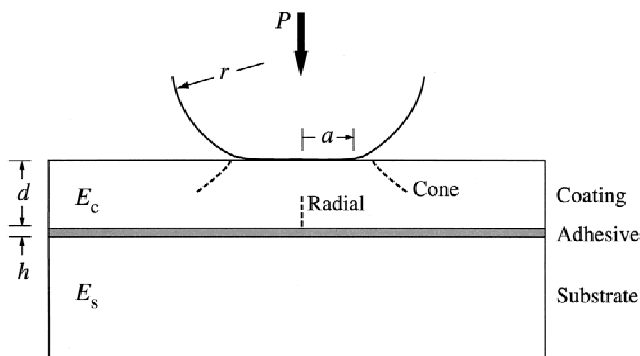


FIG. 1. Schematic diagram showing indentation setup on coating/substrate layer system bonded with thin adhesive, with ensuing cone and radial cracks.

face radial cracks, were thereby measured directly.^{14,15}

Results of the contact tests are shown in Fig. 2, as critical loads P_{cone} for cone cracking (top abraded surfaces) and P_{rad} for radial cracking (bottom abraded surfaces) versus coating/substrate Young's modulus ratio E_c/E_s , for fixed soda-lime coating thickness $d = 1.0 \text{ mm}$ and adhesive thickness $h = 10 \mu\text{m}$, and WC sphere radius $r = 3.18 \text{ mm}$. Data are plotted for cone cracks (squares) and radial cracks (circles). Each data point represents the mean and standard deviation of at least 5 indentations. The P_{cone} data show a slight rise with increasing E_c/E_s , indicating a low sensitivity of cone fracture to substrate modulus. This is consistent with a dominant contact near-field, relatively unaffected by substrate conditions, in the cone initiation process. On the other hand, the P_{rad} data show a comparatively strong decline with increasing E_c/E_s , although less so in the region of softer substrates ($E_c/E_s \gg 1$), indicating that substrate modulus is a much more important factor in this second mode of fracture. Note that the two data sets cross each other, at $E_c/E_s \approx 5$, for the values of d , h , and r used in our experiments.

The solid curves in Fig. 2 are theoretical fits to the two data sets, as follows. (i) Cone cracks. We assume that any influence of the substrate or adhesive on the contact near field is negligible. Accordingly, we use a horizontal line to approximate the $P_{\text{cone}}(E_c/E_s)$ data in Fig. 2, representing the critical load for cone fracture in a soda-lime glass monolith ($E_c/E_s = 1$). This critical load is given by classical Hertzian fracture theory,¹⁶⁻¹⁸

$$P_{\text{cone}} = ArG_c, \quad (1)$$

with G_c the crack resistance (toughness) and A a dimensionless constant. Substituting $P_{\text{cone}} = 205 \text{ N}$ for monolithic glass ($E_c/E_s = 1$), $r = 3.18 \text{ mm}$, and $G_c = 7.1 \text{ J m}^{-2}$ for soda-lime glass,¹⁹ Eq. (1) yields $A = 8.4 \times 10^3$. (ii) Radial cracks. We propose that radial cracks initiate at the bottom coating surface when the maximum tensile stress on that surface equals the bulk flexure strength σ_F

TABLE I. Composition (wt%) and modulus of glasses used in this study.

Layer	SiO ₂	Na ₂ O	K ₂ O	CaO	BaO	MgO	PbO	BeO	ZnO	Al ₂ O ₃	B ₂ O ₃	ZrO ₂	E (GPa)
Coating (glass)	75.0	15.0	...	10.0	70
Substrate (glass)	10.0	90.0	...	21
	30.0	70.0	44
	80.3	4.0	0.4	0.3	2.8	12.2	...	62
	96.6	0.02	0.4	2.9	...	68
	36.0	4.2	4.2	39.3	10.0	6.3	103
	8.1	34.8	4.0	4.1	...	38.1	4.8	6.1	109
	47.6	19.0	...	9.5	...	9.5	4.8	9.5	123
	47.4	26.0	...	12.3	...	14.2	132
Substrate (plastic)	Soft plastic												0.90
	Polycarbonate												2.35
	Acrylic												5.20

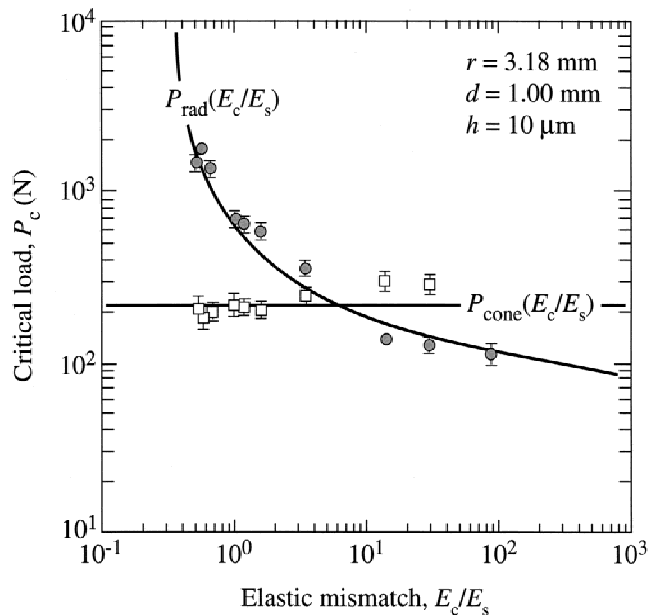


FIG. 2. Plot of critical loads P_{cone} and P_{rad} versus E_c/E_s for layer structures consisting of soda-lime glass plate coatings on various substrates of different modulus (Table I), bonded with epoxy adhesive.

of the coating.¹⁴ For small contact radius, we adopt a solution for an infinitely wide center-point-loaded slab of modulus E_c on a soft foundation,²⁰ modified to express the foundation elasticity in terms of modulus E_s ,²¹

$$P_{rad} = B\sigma_F d^2 / \log(CE_c/E_s) \quad , \quad (2)$$

in the approximation of small contacts ($a \ll d$, Fig. 1) and small surface displacements, where B and C are dimensionless coefficients. Inserting coating thickness $d = 1.00$ mm and soda-lime glass strength $\sigma_f = 110$ MPa,¹⁴ a best fit to the $P_{rad}(E_c/E_s)$ data in Fig. 2 yields $B = 2.50$ and $C = 2.84$.

No delamination failures were observed in our tests, over the range of contact loads covered.

Thus we have examined the effect of elastic modulus mismatch on the critical loads for contact-induced fracture in soda-lime glass coating layers (thickness $d = 1$ mm) bonded to relatively thick substrate layers of varied modulus by a thin layer of epoxy adhesive ($h = 10$ μ m). The data are for indentations with a WC sphere (radius $r = 3.18$ mm) and for top or bottom coating surfaces preabraded to ensure a uniform density of flaws for initiating cracks. The data in Fig. 2 demonstrate a relative insensitivity of critical load P_{cone} for surface cone cracking to elastic mismatch, E_c/E_s ; corresponding critical loads P_{rad} for subsurface radial cracking exhibit a modest sensitivity to E_c/E_s in the region of soft substrates ($E_c/E_s > 1$) but considerably higher sensitivity in the region of stiff substrates ($E_c/E_s < 1$). These trends are consistent with the modulus dependencies in Eqs. (1) and (2): zero in Eq. (1) and logarithmic in Eq. (2). Note that

the controlling material quantity in Eq. (1) is toughness, G_c , reflecting the stability conditions of crack initiation in inhomogeneous near-contact (Hertzian) fields;^{16,18} whereas in Eq. (2) it is strength, σ_F , that controls, indicative of a dominant flexure far field.¹⁴ In this context, we would note that toughness and strength do not always bear a proportional relationship. Indeed, in ceramics with crack-resistance curves the relationship can even be inverse, because incorporation of microstructural elements that confer toughness can weaken the material in the short-crack region.¹⁸

Plots such as Fig. 2 provide a useful basis for coating/substrate design. For coating surfaces with abrasion flaws on both surfaces, first cracking will depend on the elastic mismatch: in the region $E_c/E_s < 5$ (harder substrates), cone cracks will initiate first; in the region $E_c/E_s > 5$ (softer substrates), radial cracks will initiate first. Of course, for surfaces without abrasion flaws, the critical loads will be higher. But it only takes a single spurious severe flaw on either surface to lower the strength, so the curves in Fig. 2 may be considered conservative. The safest systems would appear to be those with very stiff substrates ($E_c/E_s < 1$), so as to inhibit initiation of radial fractures. However, stiffness is usually accompanied by brittleness, so that any radial cracks, once initiated, would be prone to catastrophic propagation across the coating/substrate into the substrate, even in the presence of a compliant intervening adhesive layer.²² Softer substrates, on the other hand, offer containment of coating cracks, i.e., damage tolerance, by redistributing the tensile stresses so as to confine cracks within the coating.¹⁴ Such is the case with teeth, where the outer enamel (or replacement porcelain in dental crowns) provides rigidity and wear resistance while the inner dentin provides resilience and toughness. (In this context, we may note that toughness and strength values for soda-lime glass are not too different from those of enamel and dental porcelains, and that typical maximum biting forces in dental function are $P \approx 100$ N.²³) Ideally, one seeks to operate within an “ultrasafe” region beneath the curves in Fig. 2, with increased care at $E_c/E_s > 5$ where radial cracks initiate first. Fortunately, the sensitivity to E_c/E_s is not strong in this latter region, so the choice of substrate material may not be too critical in the design specifications.

In principle, the relations in Eqs. (1) and (2) should enable extrapolation of the results to other potential coating systems, e.g., for systems with different sphere radius r and coating thickness d .¹⁴ Changing these dimensions will shift the relative positions of the curves in Fig. 2, including the crossover value of E_c/E_s at $P_{rad} = P_{cone}$. However, such extrapolations need to be made with caution—Eqs. (1) and (2) are not exact. There does appear to be a systematic, if slight, dependence of P_{cone} and hence A in Eq. (1) on elastic mismatch, indicating that

even the near-contact field is subject to influence from the substrate. In an earlier study of like, adhesively bonded soda-lime glasses ($E_c/E_s = 1$), this influence from the substrate was evident as a slight dependence of A on d .¹⁵ In that same earlier study, it was also demonstrated that B in Eq. (2) has secondary dependencies on d and h . Empirical correction factors were introduced to account for these dependencies. Note in Fig. 2 that radial cracks still initiate at $E_c/E_s \leq 1$, inconsistent with the requirement that flexural tensile stresses should vanish for monoliths [i.e., $C = 1$ at $h \rightarrow 0$ and $E_c = E_s$, resulting in $P_{\text{rad}} \rightarrow \infty$ in Eq. (2)]. In this region of stiff substrates the adhesive is solely responsible for any coating flexure. (This suggests that if we could eliminate the intervening soft adhesive altogether, e.g., by fusing the coating to the substrate, radial cracking would be eliminated in coatings on stiffer substrates.) Hence C must also depend on d and h (as well as on the relative adhesive modulus ratios E_a/E_c and E_a/E_s). The exact dependencies of the critical loads on these secondary factors are inevitably complex and may be best evaluated by numerical methods, e.g., finite-element analysis.¹⁴

In the brittle coating systems considered here, transverse cone and radial cracks are the dominant fracture modes. We have focused on just initiation conditions, in the interest of conservative design. Interface delamination cracks might be expected at more weakly bonded interfaces, especially in more severe loading conditions (e.g., repeat loading, i.e., fatigue). Other kinds of surface ring crack that initiate well outside the contact in place of the more conventional Hertzian cones may well occur in thinner coatings where flexure is enhanced.¹⁵ The more complex evolution of all these crack types in different coating structures, from initiation to final coating failure, is an area that remains to be studied.

ACKNOWLEDGMENTS

This work was supported by National Institute of Standards and Technology (NIST) internal funds and by grants from the Korea Science and Engineer-

ing Foundation (Y-W.R.) and the United States National Institute of Dental Research. Information on product names and suppliers in this paper is not to imply endorsement by NIST.

REFERENCES

1. M.V. Swain and J. Mencik, *Thin Solid Films* **253**, 204 (1994).
2. D.F. Diao, K. Kato, and K. Hokkirigawa, *Trans ASME J. Tribol.* **116**, 860 (1994).
3. L. An, H.M. Chan, N.P. Padture, and B.R. Lawn, *J. Mater. Res.* **11**, 204 (1996).
4. A. Pajares, L. Wei, B.R. Lawn, N.P. Padture, and C.C. Berndt, *Mater. Sci. Eng. A* **208**, 158 (1996).
5. S. Wuttiphan, B.R. Lawn, and N.P. Padture, *J. Am. Ceram. Soc.* **79**, 634 (1996).
6. A.C. Fischer-Cripps, B.R. Lawn, A. Pajares, and L. Wei, *J. Am. Ceram. Soc.* **79**, 2619 (1996).
7. T.J. Lardner, J.E. Ritter, and G-Q. Zhu, *J. Am. Ceram. Soc.* **80**, 1851 (1997).
8. H.M. Chan, *Ann. Rev. Mater. Sci.* **27**, 249 (1997).
9. K.S. Lee, S. Wuttiphan, X.Z. Hu, S.K. Lee, and B.R. Lawn, *J. Am. Ceram. Soc.* **81**, 571 (1998).
10. K.S. Lee, S.K. Lee, B.R. Lawn, and D.K. Kim, *J. Am. Ceram. Soc.* **81**, 2394 (1998).
11. Y.G. Jung, S. Wuttiphan, I.M. Peterson, and B.R. Lawn, *J. Dent. Res.* **78**, 887 (1999).
12. B.R. Lawn, *J. Am. Ceram. Soc.* **81**, 1977 (1998).
13. H. Zhao, X.Z. Hu, M.B. Bush, and B.R. Lawn, *J. Mater. Res.* **15**, 676 (2000).
14. H. Chai, B.R. Lawn, and S. Wuttiphan, *J. Mater. Res.* **14**, 3805 (1999).
15. H. Chai and B.R. Lawn, *J. Mater. Res.* **15**, 1017 (2000).
16. F.C. Frank and B.R. Lawn, *Proc. R. Soc. London A* **299**, 291 (1967).
17. B.R. Lawn and T.R. Wilshaw, *J. Mater. Sci.* **10**, 1049 (1975).
18. B.R. Lawn, *Fracture of Brittle Solids* (Cambridge University Press, Cambridge, United Kingdom, 1993), Chaps. 7 and 8.
19. S.M. Wiederhorn, *J. Am. Ceram. Soc.* **52**, 99 (1969).
20. S. Timoshenko and S. Woinowsky-Krieger, *Theory of Plates and Shells* (McGraw-Hill, New York, 1959), Chap. 8.
21. P.M. Ramsey, H.W. Chandler, and T.F. Page, *Surf. Coat. Technol.* **49**, 504 (1991).
22. M.C. Shaw, D.B. Marshall, M.S. Dadkhah, and A.G. Evans, *Acta Metall.* **41**, 3311 (1993).
23. I.M. Peterson, A. Pajares, B.R. Lawn, V.P. Thompson, and E.D. Rekow, *J. Dent. Res.* **77**, 589 (1998).